

Early transcriptomic response of *Alnus glutinosa* to *Frankia alni* symbiont, an upregulated nsLTP (non-specific Lipid Transfer Protein) is implicated in early and late stages of symbiosis.

Melanie GASSER¹, Nicole ALLOISIO¹, Pascale FOURNIER¹, Severine BALMAND², Ons KHARRAT¹, Joris TULUMELLO^{1£}, Aziz HEDDI², Pedro Da SILVA², Philippe NORMAND¹, Hasna BOUBAKRI^{1#}, Petar PUJIC¹

1-Université de Lyon, F-69361, Lyon, France ; Université Claude Bernard Lyon 1, CNRS, UMR 5557, INRA UMR1418, Ecologie Microbienne, F-69622, Villeurbanne, France

2-INSA-Lyon, INRA, UMR203 BF2I, Biologie Fonctionnelle Insectes et Interactions, Villeurbanne, France

#corresponding author: hasna.boubakri@univ-lyon1.fr, tel: 33-472 44 82 00

£ present address: Aix Marseille Univ, CEA, CNRS, BIAM, Lab Microbial Ecology of the Rhizosphere (LEMIRE), F-13108, Saint-Paul-Lez-Durance, France; BioIntrant 139, Rue Philippe de Girard, Pertuis F-84120, France.

Summary

The response of *Alnus glutinosa* to *Frankia alni* is complex with several sequential physiological modifications that include calcium spiking, root hair deformation, penetration, induction of primordium, formation and growth of nodule. A transcriptomic study of seedlings in hydroponics after early contact (2.5 days) with *Frankia alni*, either with a culture supernatant or with living cells separated from the roots by a dialysis

membrane, permitted to identify plant genes which expression level was modified upon early contact with *Frankia*.

Forty-two genes were significantly up-regulated in both experiments, most of them encoding biological processes such as oxidative stress or response to stimuli. Among them, the most upregulated gene was a non-specific lipid transfer protein encoding gene with a fold change of 141. This nsLTP was found to increase *Frankia* nitrogen fixation at sub-lethal concentration. Interestingly, it was immunolocalized to a region of the deformed root hair at an early infection stage and later in nodules, it was localized around bacterial vesicles suggesting a role in early and late stages of symbiosis.

Keywords: nitrogen fixation, antimicrobial peptide, immunity, root hairs, oxidative stress, lipid, infection threads, nodule

Introduction

Symbiosis between *Alnus glutinosa* and the actinobacterium *Frankia alni* permits the establishment of root nodules in which nitrogen fixation takes place. This permits alder and other plants collectively called "actinorhizal" to grow on nitrogen-poor soils and initiate ecological successions. The determinants of this interaction are poorly known, due among other reasons to the lack of a transformation system in alder. *Alnus glutinosa* is the type species of the genus (1), it grows in pioneer biotopes such as glacial moraines, volcanic ashes and mine spoils (2) and its genome has been deciphered recently (3).

The presence of a symbiotic bacterium like *Frankia* or simply that of its exudates, triggers in the host plant tissues a series of events leading to root hair deformation and calcium spiking (4). Later, penetration, primordium formation and growth of nodules follow with subsequent exchange of nutrients. Omic analyses have permitted to gain a global view of

the physiological changes taking place upon specific challenges. In particular, transcriptomics of 21 dpi (day post-inoculation) nodules permitted to see on the plant side the presence of homologs of the whole common symbiotic signalling cascade or CSSP (5, 6), some of which have been lost in non-symbiotic neighbours (3).

This important conservation on the plant side of the common symbiotic pathway (5) contrasts with the absence in most *Frankia* genomes (7) of the canonical *nod* genes which are involved in the biosynthesis of Nod Factor (NF) in majority of Rhizobia (8). In mature nodules, the bacterial genes *nif*, *hup*, *shc* and *suf* are upregulated but no trace of a symbiotic island was found (9). A study of the *Frankia alni* early response (2.5 dpi) showed that several determinants were upregulated among which a K-transporter, lipid modifying enzymes and a conserved cellulose synthase cluster (10). Proteomics was done on a related species, *Frankia coriariae* that permitted to see upregulation of cell wall remodelling enzymes, signal transduction and host signal processing proteins (11). Metabolomics on an *Alnus*-infective strain showed the presence of various compounds absent from roots (12), high levels of TCA intermediates citrate, fumarate and malate (13) and high levels of citrulline, glutamate and pyruvate (14, 15)..

Signalling between alder and *Frankia alni* involves on the part of the bacterium the synthesis of an uncharacterized root hair deforming factor (16, 17) and that of the auxin PAA (18). On the plant side, less is known besides the upregulation of defensins that modify the porosity of *Frankia* membranes (19, 20).

We undertook the present study to better understand the initial steps of the actinorhizal symbiosis on the plant side where the symbiont must be recognized to pave the way for its internalization. To analyse this early plant reaction when it perceives its symbiont, we did a cell-free contact through two conditions: indirect contact with *Frankia* trapped in dialysis tube or its supernatant and by targeting 2.5 dpi response, by which time extensive

root hair deformation has occurred (21) and before primordium formation at 7dpi (22). We further focussed on the most upregulated gene coding a non-specific Lipid Transfer Protein (nsLTP), which is also one of the most overexpressed genes in the nodule. We localized this peptide in different plant tissues and did physiological tests to decipher its biological function at early and late steps of symbiosis.

Materials and methods

Strains and growth condition before total RNA extraction

The same approach used previously (10), was used here to obtain plant samples at an early stage of infection for RNA extraction. Briefly, *Frankia alni* ACN14a (23) was grown in BAP- PCM media until log-phase, collected by centrifugation, washed twice with sterile ultra-pure water and suspended in Farhaeus medium without KNO₃. *Frankia* cells were homogenised by forced passage through a series of needles (21G, 23G, 25G, 27G) before inoculation.

Alnus glutinosa seeds obtained from a single individual growing on the banks of the river Rhone in Lyon were surface sterilised and grown as described earlier (10). Seedlings were transferred to Fåhraeus' solution (24) in opaque plastic pots (8 seedlings/ pot) and grown for four weeks with 0.5 g.L⁻¹ KNO₃, followed by one week without KNO₃ before inoculation. Two independent experiments were performed. In experiment #1 (Exp 1- *Frankia* indirect contact (FIC)), 8ml of *Frankia* cells were transferred to dialysis tubing (MWCO=100kDa) and arranged into a plastic pot containing 8 seedlings and filled with Fåhraeus' solution without KNO₃. Five biological replicates were performed with 4 plastic pots per replicate. In experiment #2 (Exp2-*Frankia* supernatant direct contact (SupC)), *Frankia* supernatants were applied directly on *Alnus* roots. Supernatant extract was prepared as follow: 250 ml log-phase culture cells were removed by centrifugation and

the supernatant filtered through 0.22 μm membranes (Millipore, Billerica, MA). Solid phase extractions of the supernatants were done using benzene sulphonic acid cation exchanger on silica (Macherey Nagel, Hoerdt, France). Elution was done using 50:50 v/v methanol-water followed by 100 % methanol. Two fractions were lyophilised under vacuum, dissolved in water and tested for root hair deformation activity on independent plant roots. In parallel, as a control condition without supernatant, an equivalent volume of culture medium was treated with the same extraction protocol. Three biological replicates were performed with 6 seedlings per replicate.

The root hair deformation process took place similarly in both direct and indirect contact conditions, confirmed with stereomicroscope observations (Leica MZ8, Wetzlar, Germany). After 2.5 days (64 hours) with root hairs highly deformed, a 2 cm long segment representing the central part of the root was cut at 2 cm from the distal end, washed with sterile water before freezing in liquid nitrogen and storing at -80°C . In addition, a T0 control condition without *Frankia* was performed and plant roots were washed and frozen as described above.

Transcriptomics of alder at 2.5dpi

Transcriptomics was done as described earlier (5). Total RNA was purified from roots using RNeasy plant mini kits (Qiagen, Courtaboeuf, France) and treated with DNases as before. Residual DNA was removed using the Turbo DNA free kit (Ambion, Thermo Fisher Scientific, Wilmington, DE), quantified using a NanoDrop spectrophotometer (Thermo Fischer Scientific) and qualitatively assessed using a Bioanalyzer 2100 (Agilent, Waldbronn, Germany).

Microarrays were designed (13909 probes; 1 probe/*A. glutinosa* unigene), manufactured and hybridised by Imaxio (<http://www.imaxio.com/index.php>), using Agilent

Technologies (<http://www.home.agilent.com/agilent/home.jspx>) as previously described (5). The microarrays were scanned with an Agilent G2505C Scanner. The Feature Extraction software (Agilent, version 11.5.1.1) was used to quantify the intensity of fluorescence signals and microarray raw data were analysed using GeneSpring GX 12.0 software (Agilent technologies). Normalisation per chip (to the 75th percentile) and per probe (to the median) were performed to allow comparison of samples. The two experiments Exp 1 and Exp 2 were analysed separately. In order to limit false positive results, microarray data were filtered according to the flag parameter “detected”. Thus, probes taken into account are uniform, non-outlying, non-saturated and displayed an intensity level above the background in at least one of the two biological conditions.

In Exp1, 1590 probes yielding an intensity level significantly below the background in the 10 samples were discarded. In addition, 1146 probes did not yield the flag “detected” in at least one of the two biological conditions and were also discarded. Thus, 11 173 probes were taken into account for subsequent analyses of Exp 1.

In Exp 2, 1765 probes yielded an intensity level significantly below the background in the 6 samples and were discarded. In addition, 1113 probes did not yield the flag “detected” in at least one of the two biological conditions and were also discarded. Thus, 11031 probes were taken into account for subsequent analyses of Exp 2. T-tests comparing *FIC* roots vs. control roots in Exp 1 and *SupC* roots vs. control roots in Exp 2 were applied and only those genes with an average fold change (FC) above 2 (up-regulated) or below 0.5 (down-regulated) with a p -value<0.05 were considered significant. The normalized and raw microarray data values have been deposited in the Gene Expression Omnibus database (www.ncbi.nlm.nih.gov/geo; accession nos. E-MTAB-8936 and E-MTAB-8937).

Quantitative real-time RT-PCR

Reverse transcription (RT) and real time quantitative PCR (qRT-PCR) were performed with the same biological replicates used for microarray experiments. For *A. glutinosa* analyses, RT was performed with 5 µg of total mRNA using Transcriptor Reverse Transcriptase and oligo (dT)₁₅ primer (Roche, Mannheim, Germany). QRT-PCR was run on a LightCycler 480 (Roche) using LightCycler 480 SYBR Green I Master (Roche) under the following conditions: 95 °C for 5 min; 45 cycles of 95 °C for 20 s, 60 °C for 20 s and 72 °C for 15 s. Primer sets were designed using ProbeFinder (Roche) and Primer 3 softwares and can be seen as Supporting Information (Table S1). Two qRT-PCR reactions were run for each biological replicate and each primer set. Expression values were normalised using the expression level of the *Ag-ubi* gene that encodes ubiquitin (5).

Cloning of *agLTP24* gene

The *agltip24* gene was PCR amplified from cDNA prepared above using designed primers (Table S1) under the following conditions: 98 °C for 30 s; 30 cycles of 98 °C for 7 s, 63 °C for 20 s and 72 °C for 8 s. The reaction mixture of 50 µl PCR contained 1X Phusion HF buffer, 200 µM dNTPs, 0.5 µM Forward primer, 0.5 µM reverse primer, 87 ng template DNA and 1-units Phusion DNA Polymerase (NEB, Evry, France). The PCR product was cloned using the hot fusion method (25) in pET30a+ vector (Merck, Molsheim France) pre-digested with *EcoRI* and *BglIII* in order to fusion AgLTP24 with a N- terminal 6XHis flag. Ligation mixture was transformed in *Escherichia coli* DH5α chemocompetent cells (26) for plasmid DNA propagation and sequencing (pET30a-HIS-AgLTP24, supplemental Fig. S1). Plasmids DNA was prepared using (Nucleospin Plasmid DNA kit Macherey Nagel) from 4 independent clones, 2 ml of each *E. coli* culture grown overnight in 5ml LB medium at 37°C with shaking. Cloned insert DNA was checked by Sanger sequencing (Biofidal,

Lyon, France) and used for electrotransformation into iShuffle T7 *lysY E. coli* cells (NEB, Evry, France), a strain used to obtain proteins with disulphide bonds (27).

AgLTP24 production and purification

Cultures were grown in LB medium supplemented with kanamycin ($40\mu\text{g}\cdot\text{ml}^{-1}$) at 30°C at 130 rpm until log phase was reached ($\text{OD}_{600} \sim 0,5$) then the HIS-AgLTP24 expression was induced with 1 mM isopropyl β -D-1-thiogalactopyranoside (IPTG). Induced cultures were incubated at 30°C for 3h at 130 rpm and harvested by centrifugation (5100 g for 10 min at 4°C). Expression was analysed by 4-20% Tricine SDS-PAGE (28). Pellets were lysed by freeze thaw and resuspended in a binding buffer (100 mM Tris, 500 mM NaCl, 5mM Imidazole, pH 7.4). A second lysis was performed using silica beads and Fastprep 24™ 5G (MP Biomedicals). The cell lysate was harvested by centrifugation at 5100 g, 4°C for 30min and used for the purification of HIS-AgLTP24 using His GravityTrap columns (GE Healthcare) with modified binding (100mM Tris, 500mM NaCl, 5mM Imidazole, pH 7.4) and elution buffers (100 mM Tris, 500 Nacl, 500 mM Imidazole, pH 7.4). Purification of HIS-AgLTP24 was verified by 4-20% Tricine SDS-PAGE. Elution fractions was applied to a 3K MWCO Amicon Ultra-15 centrifugal filter (Merck Millipore) to buffer exchange with the enterokinase buffer (20 mM Tris, 50 mM NaCl, 2 mM CaCl_2 , pH 6.8) and concentrate. The HIS tag was removed from the mature sequence of AgLTP24 with enterokinase (NEB, Evry, France) for 16 h at room temperature. Cleavage was confirmed by 4-20% Tricine SDS-PAGE. The enterokinase was removed from the mixture using the Enterokinase Removal Kit (Sigma). His tag removal was done with a His GravityTrap column (GE-Healthcare) using an imidazole free binding buffer (100 mM Tris, 500 mM NaCl, pH 7.4). Wash fractions containing AgLTP24 purified were applied to a 3K MWCO Amicon Ultra-15 centrifugal filter (Merck Millipore) for buffer exchange with NH_4^+ -free FBM medium

(FBM-). Final concentration was determined with Qubit Protein Assay Kit (ThermoFisher). The purified AgLTP24 protein were further analysed by UPLC-ESI-HRMS. The system used for UPLC-ESI-HRMS was an ultra-performance liquid chromatography Ultimate 3000 (Thermo Fisher Scientific, Villebon-sur-Yvette, France) coupled to a high resolution hybrid quadrupole-time of flight mass spectrometer (Impact II, Bruker, Brême, Germany) equipped with electrospray ionization source (ESI) (Bruker, Brême Germany). Instrument control and data collection were performed using Data Analysis 5.0 software.

Immunolocalization of AgLTP24

Immunostaining and fluorescence microscopy was done as described earlier (29) with the synthesised epitope (DKHSTADFEKLA PCGKAAQD) injected to a rabbit (Covalab). Plant immunolocalisation was performed on *A. glutinosa* roots (2.5 dpi) as described above in Exp 1 (FindC). In addition, nodules (21dpi) obtained as a previous study (19) were also used here to localise agLTP24 at the mature stage of symbiosis. T0 non-infected seedlings were used as control.

Physiological assays with AgLTP24 on *Frankia alni*.

The antimicrobial activity of AgLTP24 (using 1 μ M, 2 μ M, 5 μ M concentrations), was done using the resazurin assay in 24-well microplates (Greiner bio-one, Les Ulis, France). A 2-week-old *Frankia* ACN14a culture grown in FBM medium supplemented by 5mM of NH₄Cl (FBM+) was centrifuged at 5100 g for 15 minutes, the supernatant was removed, and the pellet homogenized in FBM- by repeated passage through syringes. *Frankia* culture was done in 1ml of FBM- per well with a final optical density of 0.02 and with an appropriate concentration of AgLTP24 peptide. Four replicates were made for each condition.

Negative (*Frankia* ACN14 in FBM-) and positive controls (*Frankia* ACN14a in FBM-supplemented by kanamycin at 40 $\mu\text{g}\cdot\text{ml}^{-1}$ final concentration) were performed. Microplates were incubated at 28°C, 80 rpm in a humid incubator. After 6 days of incubation, resazurin (Fisher Scientific SAS, Illkirch, France) was added to a final concentration of 6.25 $\mu\text{g}\cdot\text{ml}^{-1}$ in each well and the microplates were incubated at 28°C, 80 rpm for 16 hours in the dark. Fluorescence measurements were performed with a microplate reader (infinite M200PRO, TECAN) with an excitation wavelength of 530nm and an emission wavelength of 590nm. The results obtained were normalised to the mean fluorescence of the negative control. Since data were normally distributed, mean comparisons with the negative control were performed with a Student's *t*-test.

A second bioassay was made by growing *F. alni* in FBM- and incubating from 1 to 14 days at 28°C (5 replicates by kinetic point and by condition) as described previously. At each kinetic point, the effects nitrogen fixation (or ARA), respiration (IRA) and on morphology were monitored (19, 30). Since data were normally distributed or not, different statistical tests were made using GraphPad Prism 9.2.0 (GraphPad software Inc; San Diego, CA, USA).

Bioinformatics

Blast analyses and GO assignation were performed on Blast2GO v5.2 using BLASTx against NR, Gene Ontology (GOs) and Inter-ProScan (31). Fishers' exact test implemented in Blast2GO was used to identify significantly enriched GO categories. A GO category was considered significantly enriched only when the *p*-value for that category was < 0.05 after applying FDR correction. Molecular mass of proteins and their isoelectric point were calculated through the Expasy software (<https://web.expasy.org/protparam/>)

Results

Transcriptomics response of alder at 2dpi

In the first early response transcriptomic experiment (Exp 1), 300 and 225 genes were found significantly up- and down- regulated in *A. glutinosa* after 2.5 days post inoculation (dpi) of *Frankia* in a separated dialysis bag (cut off 100 KDa -*Frankia* indirect contact (FindC) roots/ control roots) by having a fold change (FC) ≥ 2 or ≤ 0.5 ($p \leq 0.05$), respectively (Table S2). In Exp2, 248 *A. glutinosa* genes were found to be significantly regulated 2.5 dpi with *Frankia* supernatant (*Frankia* supernatant contact (FsupC) roots/control roots). Of these, 176 and 76 genes were also up- and down- regulated in Exp2; respectively (Table S3). By comparing ESTs present in both experiments, 84 genes were found significantly up- or down-regulated (See SI Table S4).

Biological processes implicated in early steps of symbiosis

A GO-based analysis of the biological processes enriched in up- and down-regulated genes within each experiment yielded 12 to 23 % of genes with no Blast hit (Fig. S2). Among the sequences with a Blast hit, 8 to 14% correspond to unknown proteins and could not be associated to any biological process. The annotated sequences retrieved were distributed in 21 different processes (Fig. 1A). The presence of *Frankia* induced at an early stage a strong induction of genes involved in response to stimuli and catabolic processes among which oxidative stress (oxidase, peroxidase) and defence (chitinase, defensin, thaumatin...) were upregulated in both conditions, as well as a large portion of genes involved in nitrogen compound metabolic processes with kinases, transferases, lyases or glucosidases. Globally, the number of sequences retrieved was higher in Exp1 than Exp2 (Fig. 1A) suggesting a stronger signal detected in indirect interaction through dialysis tubing.

A statistical analysis permitted to identify certain enzyme families by comparing each pool of genes. Even this Fisher test made in both experiment, only Exp1 gave statically valid differences in GO assignation between up and down-regulated genes (Fig. 1B).

In Exp1, an overrepresentation of genes coding enzymes involved in oxidation-reduction biological processes and oxidative stress responses was seen with numerous peroxidases, catalases, oxidases or lipoxygenases overexpressed (Table S1). Also, chemical reactions involving alpha and aromatic amino acid metabolism and fatty acid beta-oxidation, selenocysteine methyltransferase, phenylalanine ammonia lyase or caffeic acid O-methyltransferase were seen following indirect contact with *Frankia* cells. Nucleotide binding proteins such as a receptor kinase (AG-N01f_037_C05), a uridine kinase (AG-N01f_030_B06) or a calcium transporting membrane (AGCL1701Contig1) were also more abundant in the set of up-regulated proteins of Exp1. Finally, several genes coding defence response were overrepresented such as endochitinase, disease resistance protein, defensin, thaumatin, allergen or nsLTP. Conversely, we observed an enrichment in down-regulated genes of one molecular function of GO assignation: isomerase such as inositol-3-phosphate synthase, ribose-5-phosphate isomerase or beta-amyrin synthase.

The most upregulated genes in both experimentations concern symbiosis

By compiling differentially regulated genes found in both experiments (Table 1 and Table S4), we compared them through GO-based analysis. An overrepresentation of only one biological process (lipid metabolism) in down-regulated genes was found with the same statistical restriction (FDR<0.05). Indeed, several genes such as synthase, reductase or oxidase and involved in triterpenoid (AG-N01f_010_H21) isopentenyl diphosphate (IPP) and dimethylallyl diphosphate (AG-N01f_014_J09); geranyl or geranylgeranyl diphosphate (GPP and GGPP) (AG-N01f_005_E08; AG-J07f_004_F15); terpene (AG-

J07f_004_M14; AGCL3086Contig1) or geranyl or geranylgeranyl diphosphate (AGCL3190Contig1) biosynthesis were detected as more abundant in down-regulated genes and already observed by our first GO assignation (Fig. 1A).

Amongst the 42 most upregulated genes found in both conditions (Table1), the most upregulated gene encodes a non-specific lipid transfer protein or nsLTP (fold changes: 140.7 (*FindC*) and 74.8 (*FsupC*)), followed by a betabutilin and a pectin methylesterase inhibitor. Remarkably, 20 out these 42 up-regulated genes encoded proteins with a peptide signal (Table 1). Among them, numerous upregulated genes encode secreted peptides (47%), some of them are classified as antimicrobial: three defensins (Ag5, Ag3 and Ag11), and a nsLTP and a thaumatin like-protein.

To confirm the level of expression at this early step, we focussed on two genes, one coding the nsLTP and the second coding the basic blue copper protein (fold changes: (fold changes: 140.7 (*FindC*) and 74.8 (*FsupC*) and 4.7 (*FindC*) and 11.7 (*FsupC*); respectively) as candidate genes for qRT-PCR with two primer pairs per gene (Table S1). Up-regulation was confirmed by qRT-PCR with the same biological replicates previously used (Table S5).

In order to follow the temporal distribution of expression, we extracted from our previous work (5) the fold change obtained with the same microarray but at 21 dpi when the nodule is formed and compared it to non-infected roots (Table 1, Fig. 2).

Almost down-regulated genes at early stage were either repressed or not modulated at nodule stage. Among them, we observed an enrichment of proteins associated to lipid metabolic process and lyase activity (Fig. 3).

Conversely, genes upregulated at 2.5 dpi are classified in three profiles. Sixteen are still induced when 17 are not modulated and 8 are repressed in nodule. For instance, genes encoding proteins involved in stress response are found in the three profiles (Fig. 3) but

we found mainly AMPs (defensin, thaumatin) in the first group when chitinase and peroxidase enriched the two other groups (Table 1). The most upregulated gene in nodule (AGCL581Contig1; FC=2941) presented also a high expression after 2.5 dpi but at moderate level (FC=8.7 and 7.1 in *FindC* and *FsupC* conditions, respectively). This gene did not give any GO annotation during our global bioinformatic analysis but a BlastN assigned it as a putative tubulin beta-2 chain like protein. In parallel, the nsLTP found as the most upregulated gene at early stage presented also a very high expression at 21 dpi (FC=2145 in nodule, Table 1) suggesting a requirement all along the symbiosis process. NsLTPs are classified as AMPs and annotated as systematic acquired resistance according GO analysis suggest its potential role in defense response. For all these reasons, we decided to focus our functional analysis on this protein.

Structure and classification of AgLTP24

The nsLTP from *A. glutinosa* overexpressed during its interaction with *Frankia* is named AgLTP24. The total nucleotide sequence is 552 base pairs and contains one exon. This sequence encodes a putative processed protein of 114 amino acids including a signal peptide with a sequence of 22 amino acids that allows its secretion [29]. The mature peptide has a molecular weight of 9700.28 Dalton and a cationic isoelectric point of 8.46, this nsLTPs is classified according to Edstam et al. (32) as Type D. It contains the characteristic motif of nsLTPs composed of 8 cysteines: C-X13-C-X14CC-X9-C-X1-C-X24-C-X10-C which stabilises the 3D structure by folding the α -helices domains with disulphide bridges forming a hydrophobic cavity.

Immunolocalization of AgLTP24 in planta

In order to determine where this nsLTP is secreted during the symbiosis, we did an immunolocalisation in plant. Antibodies anti-AgLTP24 were applied to different alder tissues inoculated or not by *Frankia*. First, we produced deformed root hairs after an indirect contact of *Frankia* (F indC) and observed signals in extracellular nooks (Fig. 3B and Fig3C). These nooks were the specific site for *Frankia* binding. No signal was detected with control rabbit serum (Fig3A) or with anti-AgLTP24 against non-infected roots (Fig. S3). Microarrays and qRT-PCR showed overexpression of this protein in mature 21 dpi nodules. We used observed a specific immunolocalisation in plant cells infected by *Frankia* situated in the fixation zone of the nodule (Fig. 3E), specifically on *Frankia*'s vesicles (Fig. 3F).

Biological production of AgLTP24

The nsLTPs are low molecular weight peptides rich in cysteines. It has a signal sequence that allows the plant to address it to a target compartment. Those nsLTPs are characterized by a conserved motif of 8 cysteines in their mature sequence forming 4 disulfide bonds important for the formation of the hydrophobic cavity, which makes their production difficult. Synthetic production is limited to small peptides with few disulfide bonds, so we developed a biological production of mature AgLTP24, i.e. without its signal peptide, in *E. coli* shuffle T7 *lysY* (Fig. S1) which are capable of forming disulfide bonds (27). We obtained a yield of 0.1mg of pure protein per litre of culture. After peptide purification, UPLC-ESI-HRMS analysis of the purified AgLTP24 protein revealed a monoisotopic [M+H]⁺ m/z 9686.8008 (theoretical monoisotopic m/z calculated for C₄₁₅H₆₇₆N₁₂₃O₁₂₆S₉: 9686.7760) consistent with the formation of four disulfide bridges (Fig. S4). This analysis was made after each run of purification and before bioassays to check the purity and the good conformation of the protein with disulphide bridges.

Physiology of *Frankia alni* in contact with AgLTP24

A miniaturised, rapid and fluorescent bioassay using resazurin dye was successfully developed to determine whether AgLTP24 had antimicrobial activity against *Frankia alni* at 7 dpi. For this, we applied a range of concentrations of AgLTP24 from 1 to 5 μ M (Fig. 4) and used kanamycin as positive control of inhibition of *Frankia*. The cell viability of *Frankia* is reduced from a concentration of 5 μ M AgLTP24 ($54 \pm 16\%$ of cell viability) while no effect was detected below this concentration. AgLTP24 can thus be considered an antibacterial peptide against the symbiotic partner at this concentration. In addition, microscopy observation showed a negative effect of AgLTP24 on vesicles' production (Fig. 4B). Indeed, at 5 μ M of AgLTP24, no vesicle was observed whereas they are present at sub-inhibitory concentrations. However, *Frankia* must be viable and efficient in the nodule to ensure nitrogen fixation for trophic exchange with its plant partner. This conducted us to perform a second physiological assay by using sub-inhibitory concentrations of AgLTP24. The second physiological assay was conducted with a range of AgLTP24 from 1nM to 1 μ M (Fig. 5). In this test, nitrogen fixation, respiratory activity (OD_{490nm}) and growth effects (OD_{600nm}) were monitored over a 10 days' time course (Fig. S5).

That range of AgLTP24 had little effect on *Frankia* growth. We noted a negative effect at 10nM of AgLTP24 on respiratory activity at early time of the time course (Fig. S5B) but it was not maintained over time. Regarding respiratory activity, we observed a positive but not significant effect with AgLTP24 above 100nM and 5 days of growth. The most striking effect was observed on nitrogen fixation after 7 days of culture (Fig. 5) with a concentration above 100nM leading to inhibitory effect whereas no effect was observed on growth or respiratory activity. Conversely, at 1nM of this peptide, the AgLTP24

improved this activity. Microscopy did show any effect on vesicle morphology (data not shown).

Discussion

Early steps of the interaction between alder and *Frankia* start with the molecular communication through the secretion of flavonoids by the plant (33, 34) and the bacterial “Nod-like” factors by *Frankia* (16, 35). This factor also called root hair deforming factor (RHDF) because it triggers plant response by reorientating root-hair tip growth followed by the formation of an infection thread (IT) and cell division induction in inner cortical cells. This process leads to a nodule where *Frankia* will be housed and exchange with its plant partner. Even though RHDF structure remains unknown, previous studies have shown that this factor of around 3KDa is present in *Frankia* cell free supernatant and acts at nanomolar dose (36). In addition, this factor is able to induce a high frequency nuclear Ca²⁺ spiking (4). Due to the lack of a genetic transformation system for alder, other approaches besides genetic inactivation have been used to identify the host symbiotic determinants.

Focusing at nodule step (5), transcriptomic analysis showed that the common symbiotic cascade known in Legumes (interacting with rhizobia) and in most land plants (interacting with VAM fungi) (37) was also present in actinorhizal plants (5, 6, 38). Previously, differential screening of cDNA libraries from root and nodules of *Alnus glutinosa* with nodule and root cDNAs permitted to identify several symbiotic genes among which a subtilisin-like protease (39), a sucrose synthase, an enolase (40), and a dicarboxylate transporter (41). These genes are evocative of tissue reorganization and trophic exchanges but shed no light on the triggering of organogenesis. The present study

was aimed at investigating the plant molecular response in early symbiotic steps by using same transcriptomic microarray as in our previous work at nodule step (5).

Global plant response at early step of symbiosis

Firstly, the two experiments induced different level of response in the plant partners with stronger signal in the Exp1 suggesting that even though the supernatant is sufficient to trigger root-hair deformation, a sustained dynamic of interaction with *Frankia* is more efficient. These results suggest that *Frankia* secretome produced during Exp1 could be more diverse triggering a strong perception of its presence by plant. Indeed, *Frankia* secretes a variety of proteolytic enzymes such as glycosidases, esterases, or proteases presumably involved in root infection (42).

Plant global response reveals a common pattern with a strong modulation of genes involved in stress response. This biological process, specific to early response (5) is constituted by genes encoding putative proteins involved in oxidative stress (oxidase, peroxidase); to defense against pathogens such as pathogenesis related (PR) proteins (chitinase, Defensin, thaumatin or nsLTP). Beside these biological processes, we can propose different steps in the plant response after *Frankia* contact.

Oxidative burst in hairy roots repressed in nodule

Focusing on oxidative stress, both the overall GO analysis showed a strong induction of genes involved in oxido-reduction metabolism (oxidase, peroxidase). These enzymes intervene in oxidative stress to reduce reactive oxygen species (ROS) suggesting that *Frankia* supernatant induces a ROS stress such as previously observed for rhizobia at early steps of interaction (43, 44). In legume roots, the enzymatic activities of catalase, ascorbate peroxidase, glutathione reductase or NADPH oxidase significantly increase

upon inoculation with bacterial symbiont (43-46). After this important release, ROS production reduced drastically to prevent root hair curling and IT formation (47, 48).

To follow this dynamics of expression over the course of symbiosis establishment, we extracted transcriptional data from our previous work made at nodule step (5). Few genes are not modulated or repressed in the nodule steps (Table S4, Fig. 2) suggesting a similar profile. Consequently, plant after *Frankia* internalization would repress this stress response but the measure of ROS abundance over the time course of the symbiosis is necessary to support this tendency.

Perception of Frankia factor, signaling and hormonal function

Little is known about the symbiotic signals produced by *Frankia* but their perception requires plant receptor. Here, a statistical analysis revealed a moderate overrepresentation of gene involved in signal transduction (Table 1; AG-N01f_037_C05) encoding a putative receptor like kinase (RLK) somewhat repressed in the nodule suggesting its potential implication in *Frankia* recognition. However, other RLK similar to Lys6/Lys7/Nfr1 of legume NF receptors (AG-R01f_025_F02) already found in *A. glutinosa* (5) are not modulated after 2.5 days, which raises the question of *Frankia* recognition. Plant RLKs have been shown to control the initiation, development, and maintenance of symbioses with beneficial mycorrhizal fungi and rhizobia (49, 50) but the mechanism in actinorhizal symbiosis remain unknown (51).

The CSSP transduction will trigger primordium organogenesis where hormonal balance plays a crucial function and particularly auxin. Indeed, exogenous auxins treatments lead to the formation of thick lateral roots resembling nodules in actinorhizal Fagales (18, 52) and an auxin influx inhibitor perturbs the formation of nodules in another actinorhizal model, *Casuarina glauca* (53). Transcriptional data at early steps sustain the pivotal

function of auxin by demonstrating the overexpression of several genes encoding auxin binding proteins (Table 1: AGCL1169Contig1) or auxin inducing proteins (Table S2: AGCL1376Contig1; AG-N01f_043_C20). We did not detect genes involved in salicylic acid (SA) or jasmonic acid (JA) biosynthesis in early steps of symbiosis however a fine bioinformatics study of metabolic routes using the genome alder is required to facilitate putative assignment and to validate or not their absence in those omic data.

In any case, perception of pathogen by plant triggers SA and JA accumulation and leads to the accumulation of PR proteins to minimize pathogen load or disease onset. In legume symbiosis, those hormones inhibit bacterial infection and nodule development (54) suggesting that NF recognition represses this accumulation.

Defense mechanisms activation

After oxidative burst, following *Frankia* contact, alder activates numerous genes encoding PR proteins which are key components of plant innate immune system against both biotic and abiotic stresses (55). More precisely, PR proteins have diverse functions such as glucanase, chitinases, thaumatin like, peroxidases, defensins, nsLTPs or thionins.

We found numerous upregulated chitinases as observed in in legumes (56-58) and described as important for rhizobia infection and IT formation (59). Also, genes for oxidative stress and chitinases are not modulated or repressed in late step of actinorhizal symbiosis (Table S4, Fig. 2) suggesting they are important in the early steps of *Frankia* infection.

Furthermore, genes encoding one uncharacterized PR proteins is upregulated after *Frankia* contact (AG-R01f_016_N10) and rapidly repressed at nodule step (Table 1). A similar profile was observed for PR10 in *M. trunculata* when associated to symbiont or pathogen infection, it is activated but in symbiotic pathway, its expression is transitory

suggesting that defense signaling pathways are suppressed during the establishment of symbiosis (60). Here, the transitory activation of the Alder PR protein could be also induced by *Frankia* factors even though a specific response must be demonstrated by comparing to other biotic and abiotic stresses.

Some of the PR proteins are classified as AMPs based on their small size, the conservation of cysteine rich motif and their potential action as antimicrobial compound (61). In alder transcriptome, we distinguished the overexpression of gene encoding plant defensins (Ag3, Ag5 and Ag11), thaumatins (AG-N01f_038_P13) and nsLTPs (AGCL115Contig1). Here, all AMPs induced at early steps are still overexpressed in nodule (Table S4, Fig. 2). Like defensin, thaumatin like proteins considered as a member of defense protein but also in plant development (62) is overinduced in alder during actinorhizal symbiosis. This expression profile is quite different to the well-documented thaumatin like gene in soybean. Indeed, the *rj4* thaumatin like gene was described as constitutively and similarly transcribed in roots and nodules and intervene at a very early stage of IT formation to inhibit nodule formation with an incompatible strain (63). This suggests that thaumatin-like proteins in alder could intervene in incompatibility function but its overexpression in nodule step also raise question about another function in nodule organogenesis.

In parallel to PR protein, several genes involved in secondary metabolism are modulated (Fig. 1) such as genes involved in biosynthesis terpene/terpenoid/steroid precursors (IPP, GPP or GGPP) are repressed during *Frankia* infection. However, those compounds were emitted by plant to repress pathogen attacks (64). Their repression in alder could permit to open a window of disarmament to allow *Frankia* cell integrity before its adhesion and internalization. However, this hypothesis has to be confirmed by metabolomics analysis of roots exudates before and after *Frankia* contact to evaluate the composition and effect those on the bacterial symbiont.

AgLTP24: from *Frankia* infection to nodule functioning

Function at early step

Global omic approach made at early steps of alder symbiosis pointed to a strong signal from one protein belonging to nsLTPs family named here AgLTP24. The immunolocalisation on curled hairy roots induced after *Frankia* contact showed the specific binding of AgLTP24 in nooks (Fig. 3) where *Frankia* embedding before internalization through IT formation. This suggests that AgLTP24 intervene in infection at early phase. This is supported by the characterization of one nsLTP (MtN5) in *M. trunculata* which induced at early stage of symbiosis and in the nodule (65, 66). Because its silencing resulted in an increased number of curling events with a reduced number of invading primordia, whereas its overexpression resulted in an increased number of nodules, authors concluded that MtN5 is important at very early step of infection for the successful establishment of the symbiotic interaction but not in nodule formation (67). Similar to MtN5 (65), AgLTP24 possesses a slight antimicrobial activity *in vitro* against its symbiont at 5 μ M. As *Frankia* cell integrity must be preserved for infection, we hypothesize that AgLTP24 concentration in contact with *Frankia* must be below to 5 μ M. Further investigation to assess protein concentration in plant tissues is a great challenge but requires the development of high-performance mass spectrometry technology coupled to imagery (68, 69).

Finally, AgLTP24 could intervene at early step of symbiosis to transduce signal within plant roots to permit IT formation as well as induce stress response in *Frankia* cells.

Function at late step

AgLTP24 is also present in nodule (Table 1) and targets specifically *Frankia's* vesicle in nodule fixation zone (Fig. 3F) but this localization is different from MtN5 binding in the distal zone of the nodule (66). However, a nsLTP (AsE246) found in *Astragalus sinicus* specifically symbiosome membranes through binding a lipid component: digalactosyldiacylglycerol (DGG) (70). In this model, the *asE246* silencing impacts nodule development with fewer matured infected plant cells.

Thus, *AgLTP24* could fix vesicle wall composed by a multilamellate hopanoid lipid envelopes (71, 72) or plant perisymbiotic membrane coating *Frankia* cells in nodule. The perisymbiosome membrane composition is less documented but non-inoculated *Alnus rubra* roots are mainly composed of glycerol, phosphatidylethanolamine, phosphatidylserine and phosphatidylcholine (73). A lipidomic study in *A. glutinosa* roots using recent technology followed by a bioassay binding is a great perspective to decipher *AgLTP24* mechanisms involved.

As observed *in vitro*, *AgLTP24* could act as antimicrobial compound by reducing cell viability and vesicles formation of *Frankia* (Fig. 4) suggesting a potential role by controlling *Frankia* proliferation in nodule. However, because expression of nitrogen fixation gene cluster is more active in symbiotic conditions compared to N-free culture condition (9, 74), the concentration probably present in the nodule fixation zone would be lower to this lethal concentration. It is worth to note that at 1nM concentration of *AgLTP24*, the nitrogen fixation activity is induced a higher but not statistically so significant without perturbing *Frankia* growth (Fig. 5). The improvement of nitrogen fixation was also observed for the *AgDef5* defensin translocated by *A. glutinosa* to *Frankia's* vesicle in nodule (19).

In addition, this defensin is also upregulated at 2.5 dpi (Table 1) suggesting the plant could deliver a cocktail of molecules including *AgLTP24* to improve bacterial infection and

nitrogen fixation in nodule. A depth investigation of this synergic effect *in vitro* opens a new perspective in addition to their genetic silencing in plant as an exciting challenge to complete the gap of knowledge regarding their role in actinorhizal symbiosis.

Contribution

Melanie GASSER (Physiology of LTP on *Frankia*, cloning, LTP purification and production, Immunoassays, statistics), Nicole ALLOISIO (Transcriptomics), Pascale FOURNIER (Biological assay on *Frankia*, Transcriptomics), Severine BALMAND (Immunoassays), Ons KHARRAT (Physiology of LTP on *Frankia*), Joris TULUMELLO (developing bioassays), Aziz HEDDI, Pedro Da SILVA (Mass spectrometry of LTP), Philippe NORMAND (Transcriptomics, writing), Hasna BOUBAKRI (Bioinformatic analysis of Omic data, Immunoassays, writing), Petar PUJIC (Biological assay for transcriptomics, LTP purification)

Acknowledgements

Thanks are expressed to Elise Lacroix and the Greenhouse facility (FR 41), to Danis Abrouk in the ibio platform for help in submission of omic data to international database, Jonathan Gervais in the AME platform to access ARA measurement and Philippe Bulet for his technical advice on peptide purification. We thank the PGE platform for other measurements. EC2CO (CNRS) and FR BioEnviSanté funding supported this work.

Bibliography

1. Navarro E, Bousquet J, Moiroud A, Munive A, Piou D, Normand P. Molecular phylogeny of *Alnus* (Betulaceae), inferred from nuclear ribosomal DNA ITS sequences. *Plant and Soil*. 2003;254(1):207-17.

2. Normand P, Fernandez MP. *Frankia*. Bergey's Manual of Systematics of Archaea and Bacteria: (eds W.B. Whitman, F.A. Rainey, P. Kämpfer, M.E. Trujillo, P. DeVos, B. Hedlund and S. Dedysh); 2019. p. 1-19.
3. Griesmann M, Chang Y, Liu X, Song Y, Haberer G, Crook MB, et al. Phylogenomics reveals multiple losses of nitrogen-fixing root nodule symbiosis. *Science*. 2018;361(6398):eaat1743.
4. Granqvist E, Sun J, Op den Camp R, Pujic P, Hill L, Normand P, et al. Bacterial-induced calcium oscillations are common to nitrogen-fixing associations of nodulating legumes and nonlegumes. *New Phytol*. 2015;207(3):551-8.
5. Hocher V, Alloisio N, Auguy F, Fournier P, Doumas P, Pujic P, et al. Transcriptomics of actinorhizal symbioses reveals homologs of the whole common symbiotic signaling cascade. *Plant Physiol*. 2011;156(2):700-11.
6. Hocher V, Alloisio N, Bogusz D, Normand P. Early signaling in actinorhizal symbioses. *Plant signaling & behavior*. 2011;6(9):1377-9.
7. Normand P, Lapierre P, Tisa LS, Gogarten JP, Alloisio N, Bagnarol E, et al. Genome characteristics of facultatively symbiotic *Frankia* sp. strains reflect host range and host plant biogeography. *Genome Res*. 2007;17(1):7-15.
8. D'Haese W, Holsters M. Nod factor structures, responses, and perception during initiation of nodule development. *Glycobiology*. 2002;12(6):79R-105R.
9. Alloisio N, Queiroux C, Fournier P, Pujic P, Normand P, Vallenet D, et al. The *Frankia alni* symbiotic transcriptome. *Mol Plant Microbe Interact*. 2010;23(5):593-607.
10. Pujic P, Alloisio N, Fournier P, Roche D, Sghaier H, Miotello G, et al. Omics of the early molecular dialogue between *Frankia alni* and *Alnus glutinosa* and the cellulase synton. *Environmental Microbiology*. 2019;0(0).
11. Ktari A, Gueddou A, Nouioui I, Miotello G, Sarkar I, Ghodhbane-Gtari F, et al. Host Plant Compatibility Shapes the Proteome of *Frankia coriariae*. *Front Microbiol*. 2017;8:720.
12. Hay AE, Boubakri H, Buonomo A, Rey M, Meiffren G, Cotin-Galvan L, et al. Control of endophytic *Frankia* sporulation by *Alnus* nodule metabolites. *Mol Plant Microbe Interact*. 2017;30:205-14.
13. Carro L, Persson T, Pujic P, Alloisio N, Fournier P, Boubakri H, et al. Organic acids metabolism in *Frankia alni*. *Symbiosis*. 2015;70(1):37-48.
14. Brooks JM, Benson DRJS. Comparative metabolomics of root nodules infected with *Frankia* sp. strains and uninfected roots from *Alnus glutinosa* and *Casuarina cunninghamiana* reflects physiological integration. *Symbiosis*. 2016;70(1):87-96.
15. Hay A-E, Herrera-Belaroussi A, Rey M, Fournier P, Normand P, Boubakri H. Feedback Regulation of N Fixation in *Frankia*-*Alnus* Symbiosis Through Amino Acids

Profiling in Field and Greenhouse Nodules. *Molecular Plant-Microbe Interactions*®. 2020;33(3):499-508.

16. C er monie H, Debell  F, Fernandez MP. Structural and functional comparison of Frankia root hair deforming factor and rhizobia Nod factor. *Canadian Journal of Botany*. 1999;77(9):1293-301.

17. Ghelue MV, L vaas E, Ring  E, Solheim B. Early interactions between *Alnus glutinosa* and Frankia strain Arl3. Production and specificity of root hair deformation factor(s). *Physiologia Plantarum*. 1997;99(4):579-87.

18. Hammad Y, Nalin R, Marechal J, Fiasson K, Pepin Rg, Berry AM, et al. A possible role for phenyl acetic acid (PAA) on *Alnus glutinosa* nodulation by Frankia. *Plant Soil*. 2003;254(1):193-205.

19. Carro L, Pujic P, Alloisio N, Fournier P, Boubakri H, Hay AE, et al. *Alnus* peptides modify membrane porosity and induce the release of nitrogen-rich metabolites from nitrogen-fixing *Frankia*. *ISME J*. 2015;9(8):1723-33.

20. Carro L, Pujic P, Alloisio N, Fournier P, Boubakri H, Poly F, et al. Physiological effects of major up-regulated *Alnus glutinosa* peptides on Frankia sp. ACN14a. *Microbiology*. 2016;162(7):1173-84.

21. Berry AM, Torrey JG. Root hair deformation in the infection process of *Alnus rubra*. *Botany*. 1983;61:2863-76.

22. Lalonde M. Immunological and Ultrastructural Demonstration of Nodulation of the European *Alnus glutinosa* (L.) Gaertn. Host Plant by an Actinomycetal Isolate from the North American *Comptonia peregrina* (L.) Coult. Root Nodule. *Botanical Gazette*. 1979;140:S35-S43.

23. Normand P, Lalonde M. Evaluation of *Frankia* strains isolated from provenances of two *Alnus* species. *Canadian Journal of Microbiology*. 1982;28(10):1133-42.

24. Fahraeus G. The infection of clover root hairs by nodule bacteria studied by a simple glass slide technique. *J Gen Microbiol*. 1957;16(2):374-81.

25. Fu C, Donovan WP, Shikapwashya-Hasser O, Ye X, Cole RH. Hot Fusion: an efficient method to clone multiple DNA fragments as well as inverted repeats without ligase. *PLoS One*. 2014;9(12):e115318.

26. Chung CT, Niemela SL, Miller RH. One-step preparation of competent *Escherichia coli*: transformation and storage of bacterial cells in the same solution. *Proc Natl Acad Sci U S A*. 1989;86(7):2172-5.

27. Lobstein J, Emrich CA, Jeans C, Faulkner M, Riggs P, Berkmen M. SHuffle, a novel *Escherichia coli* protein expression strain capable of correctly folding disulfide bonded proteins in its cytoplasm. *Microbial cell factories*. 2012;11:56-.

28. Schagger H. Tricine-SDS-PAGE. *Nat Protoc*. 2006;1(1):16-22.

29. Login FH, Balmand S, Vallier A, Vincent-Monégat C, Vigneron A, Weiss-Gayet M, et al. Antimicrobial peptides keep insect endosymbionts under control. *Science*. 2011;334(6054):362-5.
30. Prin Y, Neyra M, Diem HG. Estimation of *Frankia* growth using Bradford protein and INT reduction activity estimations: application to inoculum standardization. *FEMS Microbiology Letters*. 1990;69(1-2):91-5.
31. Conesa A, Gotz S. Blast2GO: A comprehensive suite for functional analysis in plant genomics. *Int J Plant Genomics*. 2008;2008:619832.
32. Edstam MM, Viitanen L, Salminen TA, Edqvist J. Evolutionary history of the non-specific lipid transfer proteins. *Mol Plant*. 2011;4(6):947-64.
33. Benoit LF, Berry AM. Flavonoid-like compounds from seeds of red alder (*Alnus rubra*) influence host nodulation by *Frankia* (Actinomycetales). *Physiologia Plantarum*. 1997;99(4):588-93.
34. Hughes M, Donnelly C, Crozier A, Wheeler CT. Effects of the exposure of roots of *Alnus glutinosa* to light on flavonoids and nodulation. *Canadian Journal of Botany*. 1999;77(9):1311-5.
35. Perrine-Walker F, Gherbi H, Imanishi L, Hocher V, Ghodhbane-Gtari F, Lavenus J, et al. Symbiotic signaling in actinorhizal symbioses. *Curr Protein Pept Sci*. 2011;12(2):156-64.
36. Cissoko M, Hocher V, Gherbi H, Gully D, Carré-Mlouka A, Sane S, et al. Actinorhizal Signaling Molecules: *Frankia* Root Hair Deforming Factor Shares Properties With NIN Inducing Factor. *Frontiers in Plant Science*. 2018;9(1494).
37. Genre A, Russo G. Does a common pathway transduce symbiotic signals in plant-microbe interactions? *Front Plant Sci*. 2016;7:96.
38. Gherbi H, Markmann K, Svistoonoff S, Estevan J, Autran D, Giczey G, et al. SymRK defines a common genetic basis for plant root endosymbioses with arbuscular mycorrhiza fungi, rhizobia, and Frankiacteria. *Proc Natl Acad Sci U S A*. 2008;105(12):4928-32.
39. Ribeiro A, Akkermans AD, van Kammen A, Bisseling T, Pawlowski K. A nodule-specific gene encoding a subtilisin-like protease is expressed in early stages of actinorhizal nodule development. *Plant Cell*. 1995;7(6):785-94.
40. van Ghelue M, Ribeiro A, Solheim B, Akkermans AD, Bisseling T, Pawlowski K. Sucrose synthase and enolase expression in actinorhizal nodules of *Alnus glutinosa*: comparison with legume nodules. *Mol Gen Genet*. 1996;250(4):437-46.
41. Jeong J, Suh S, Guan C, Tsay YF, Moran N, Oh CJ, et al. A nodule-specific dicarboxylate transporter from alder is a member of the peptide transporter family. *Plant Physiol*. 2004;134(3):969-78.

42. Mastrorunzio JE, Tisa LS, Normand P, Benson DR. Comparative secretome analysis suggests low plant cell wall degrading capacity in *Frankia* symbionts. *BMC Genomics*. 2008;9:47.
43. Peleg-Grossman S, Melamed-Book N, Levine A. ROS production during symbiotic infection suppresses pathogenesis-related gene expression. *Plant signaling & behavior*. 2012;7(3):409-15.
44. Peleg-Grossman S, Golani Y, Kaye Y, Melamed-Book N, Levine A. NPR1 protein regulates pathogenic and symbiotic interactions between *Rhizobium* and legumes and non-legumes. *PLoS One*. 2009;4(12):e8399.
45. Bueno P, Soto MJ, Rodríguez-Rosales MP, Sanjuan J, Olivares J, Donaire JP. Time-course of lipoxygenase, antioxidant enzyme activities and H₂O₂ accumulation during the early stages of *Rhizobium*-legume symbiosis. *New Phytologist*. 2001;152(1):91-6.
46. Den Herder J, Lievens S, Rombauts S, Holsters M, Goormachtig S. A Symbiotic Plant Peroxidase Involved in Bacterial Invasion of the Tropical Legume *Sesbania rostrata* *Plant Physiology*. 2007;144(2):717-27.
47. Lohar DP, Haridas S, Gantt JS, VandenBosch KA. A transient decrease in reactive oxygen species in roots leads to root hair deformation in the legume-rhizobia symbiosis. *New Phytol*. 2007;173(1):39-49.
48. Shaw SL, Long SR. Nod factor inhibition of reactive oxygen efflux in a host legume. *Plant physiology*. 2003;132(4):2196-204.
49. Buendia L, Girardin A, Wang T, Cottret L, Lefebvre B. LysM Receptor-Like Kinase and LysM Receptor-Like Protein Families: An Update on Phylogeny and Functional Characterization. *Frontiers in Plant Science*. 2018;9(1531).
50. Chiu CH, Paszkowski U. Receptor-Like Kinases Sustain Symbiotic Scrutiny1 [OPEN]. *Plant Physiology*. 2020;182(4):1597-612.
51. Svistoonoff S, Hoher V, Gherbi H. Actinorhizal root nodule symbioses: what is signalling telling on the origins of nodulation? *Curr Opin Plant Biol*. 2014;20C:11-8.
52. Svistoonoff S, Laplaze L, Auguy F, Runions J, Duponnois R, Haseloff J, et al. cg12 expression is specifically linked to infection of root hairs and cortical cells during *Casuarina glauca* and *Allocasuarina verticillata* actinorhizal nodule development. *Mol Plant Microbe Interact*. 2003;16(7):600-7.
53. Peret B, Svistoonoff S, Lahouze B, Auguy F, Santi C, Doumas P, et al. A Role for auxin during actinorhizal symbioses formation? *Plant Signal Behav*. 2008;3(1):34-5.
54. Liu H, Zhang C, Yang J, Yu N, Wang E. Hormone modulation of legume-rhizobial symbiosis. *Journal of Integrative Plant Biology*. 2018;60(8):632-48.
55. Ali S, Ganai BA, Kamili AN, Bhat AA, Mir ZA, Bhat JA, et al. Pathogenesis-related proteins and peptides as promising tools for engineering plants with multiple stress tolerance. *Microbiological Research*. 2018;212-213:29-37.

56. Xie Z-P, Staehelin C, Wiemken A, Broughton WJ, Müller J, Boller T. Symbiosis-stimulated chitinase isoenzymes of soybean (*Glycine max* (L.) Merr.). *Journal of Experimental Botany*. 1999;50(332):327-33.
57. Goormachtig S, Lievens S, Van de Velde W, Van Montagu M, Holsters M. Srchi13, a Novel Early Nodulin from *Sesbania rostrata*, Is Related to Acidic Class III Chitinases. *The Plant Cell*. 1998;10(6):905-15.
58. Staehelin C, Granado J, Müller J, Wiemken A, Mellor RB, Felix G, et al. Perception of *Rhizobium* nodulation factors by tomato cells and inactivation by root chitinases. *Proceedings of the National Academy of Sciences*. 1994;91(6):2196-200.
59. Malolepszy A, Kelly S, Sørensen KK, James EK, Kalisch C, Bozsoki Z, et al. A plant chitinase controls cortical infection thread progression and nitrogen-fixing symbiosis. *Elife*. 2018;7:e38874.
60. Chen T, Duan L, Zhou B, Yu H, Zhu H, Cao Y, et al. Interplay of Pathogen-Induced Defense Responses and Symbiotic Establishment in *Medicago truncatula*. *Frontiers in microbiology*. 2017;8:973-.
61. Tam JP, Wang S, Wong KH, Tan WL. Antimicrobial Peptides from Plants. *Pharmaceuticals*. 2015;8(4):711-57.
62. de Jesús-Pires C, Ferreira-Neto JRC, Pacifico Bezerra-Neto J, Kido EA, de Oliveira Silva RL, Pandolfi V, et al. Plant Thaumatin-like Proteins: Function, Evolution and Biotechnological Applications. *Curr Protein Pept Sci*. 2020;21(1):36-51.
63. Hayashi M, Shiro S, Kanamori H, Mori-Hosokawa S, Sasaki-Yamagata H, Sayama T, et al. A Thaumatin-Like Protein, Rj4, Controls Nodule Symbiotic Specificity in Soybean. *Plant and Cell Physiology*. 2014;55(9):1679-89.
64. Cheng A-X, Lou Y-G, Mao Y-B, Lu S, Wang L-J, Chen X-Y. Plant Terpenoids: Biosynthesis and Ecological Functions. *Journal of Integrative Plant Biology*. 2007;49(2):179-86.
65. Pii Y, Astegno A, Peroni E, Zaccardelli M, Pandolfini T, Crimi M. The *Medicago truncatula* N5 gene encoding a root-specific lipid transfer protein is required for the symbiotic interaction with *Sinorhizobium meliloti*. *Mol Plant Microbe Interact*. 2009;22(12):1577-87.
66. Pii Y, Molesini B, Masiero S, Pandolfini T. The non-specific lipid transfer protein N5 of *Medicago truncatula* is implicated in epidermal stages of *rhizobium*-host interaction. *BMC Plant Biol*. 2012;12:233.
67. Pii Y, Molesini B, Pandolfini T. The involvement of *Medicago truncatula* non-specific lipid transfer protein N5 in the control of rhizobial infection. *Plant signaling & behavior*. 2013;8(7):e24836-e.
68. Gemperline E, Keller C, Jayaraman D, Maeda J, Sussman MR, Ané JM, et al. Examination of Endogenous Peptides in *Medicago truncatula* Using Mass Spectrometry Imaging. *J Proteome Res*. 2016;15(12):4403-11.

69. Gemperline E, Jayaraman D, Maeda J, Ane JM, Li L. Multifaceted investigation of metabolites during nitrogen fixation in *Medicago* via high resolution MALDI-MS imaging and ESI-MS. *J Am Soc Mass Spectrom*. 2015;26(1):149-58.
70. Lei L, Chen L, Shi X, Li Y, Wang J, Chen D, et al. A Nodule-Specific Lipid Transfer Protein AsE246 Participates in Transport of Plant-Synthesized Lipids to Symbiosome Membrane and Is Essential for Nodule Organogenesis in Chinese Milk Vetch. *Plant Physiology*. 2014;164(2):1045-58.
71. Berry AM, Harriott OT, Moreau RA, Osman SF, Benson DR, Jones AD. Hopanoid lipids compose the *Frankia* vesicle envelope, presumptive barrier of oxygen diffusion to nitrogenase. *Proceedings of the National Academy of Sciences*. 1993;90(13):6091-4.
72. Nalin R, Putra S, Domenach AM, Rohmer M, Gourbière F, Berry A. High hopanoid/total lipids ratio in *Frankia* mycelia is not related to the nitrogen status. *Microbiology*. 2000;146 (Pt 11):3013-9.
73. Berry AM, Moreau RA, Jones AD. Bacteriohopanetetrol: abundant lipid in *Frankia* cells and in nitrogen-fixing nodule tissue. *Plant Physiol*. 1991;95(1):111-5.
74. Lurthy T, Alloisio N, Fournier P, Anchisi S, Normand P, Pujic P, et al. Molecular response to nitrogen starvation by *Frankia alni* ACN14a revealed by transcriptomics and functional analysis with a fosmid library in *Escherichia coli*. *Research in Microbiology* 2018.

Table 1: The up-regulated genes during early root hair deformation of *Alnus glutinosa* in both experiments, with *Frankia* indirect contact (FIndC) and with *Frankia* supernatant contact (FSupC)

For contigs, EMBL-Accession numbers of all the contigated EST sequences are indicated.
 Singleton or contig nucleotide sequences are indicated when they were not of high-enough quality for EMBL submission acceptance.
 Fold Change (FC) is the ratio between FIndC roots and control roots and between FSupC roots and control roots, respectively.

The significant difference of gene expression between FIndC roots and control roots and between FSupC roots and control roots (FC ≥ 2 or ≤ 0.05) was assessed by a T-test at $p < 0.05$

*: Results of the previously reported microarray study with *Alnus glutinosa* nodules are indicated: FC* is the ratio between nodules and non inoculated root and p* is the p value of a T-student test comparing these two conditions (Hoher et al., 2011). ns indicated non significant difference between nodules and non inoculated root (p < 0.05)

For EMBL-accession number, see Suppl Table 3.

**-AGCL3038Ccontig1 sequence is the 3' non coding region of basic blue copper gene (AG-N01F_023_115).

Clone Name	<i>Frankia</i> indirect contact (FIndC)		<i>Frankia</i> supernatant contact (FSupC)		Nodule*		Sequence homology	GO annotation	Peptide signal	Theoretical pI/Mw	
	FC	p < 0.05	FC	p < 0.05	FC*	p*					
AGCL115Ccontig1	140.65	1.78E-06	74.8	1.12E-05	2145.65	1.38E-02	lipid transfer protein	systemic acquired resistance	Yes	8.46 / 9700.28	
AG-N01F_017_D15	24.72	1.72E-06	11.7	2.09E-03	172.71	5.66E-03	betatubulin 14	microtubule-based process	No	ND	
AG-R01F_023_D12	10.02	3.30E-04	8.4	3.79E-04	0.55	NS	pectin methyltransferase inhibitor	pectinesterase inhibitor activity	Yes	4.41 / 16267.16	
AGCL58Ccontig1	8.78	5.70E-04	7.1	4.17E-03	2941.04	7.08E-04	NA		0	10.07 / 11702.98*	
AGCL3639Ccontig1	8.57	1.35E-05	3.1	1.66E-02	55.49	9.27E-03	NA		0	?	
AG-R01F_043_B03	7.89	4.73E-04	12.0	6.70E-03	0.90	NS	Major pollen allergen Ah g 1	cellular response to stimulus	No	5.57 / 15622.87	
AG-R01F_030_G24	7.07	4.26E-08	17.4	5.13E-04	288.39	4.27E-03	plant basic secretory protein (BSP), peptidase M		0	Yes	ND
AG-N01F_038_P13	7.06	3.27E-04	2.9	1.54E-02	9.13	1.52E-02	thumatin like protein precursor		0	Yes	ND
AGCL3713Ccontig1	6.77	5.79E-03	4.1	1.27E-02	155.02	1.24E-03	defensin cysteine rich antimicrobial protein, Ag5	cellular response to stimulus	Yes	9.22 / 8145.27	
AGCL1289Ccontig1	6.04	4.08E-08	2.9	2.15E-03	1.56	6.22E-03	proline-rich extensin-related protein-like		0	Yes	9.60 / 16039.35
AG-R01F_030_E08	6.04	4.68E-04	3.4	7.87E-03	46.10	1.19E-02	defensin cysteine rich antimicrobial protein, Ag11	cellular response to stimulus	Yes	7.01 / 6276.13	
AGCL3038Ccontig1	5.67	4.96E-06	11.3	2.83E-04	31.43	4.86E-03	3' non coding region of basic blue copper gene	oxidation-reduction process	0	Non coding region	ND
AGCL649Ccontig1	5.21	1.80E-05	2.3	8.49E-03	0.43	3.64E-03	class II peroxidase		Yes	ND	
AGCL1440Ccontig1	5.20	9.33E-06	2.2	2.81E-02	1.01	NS	chitinase / Hevein / PR-4 / Wheatwin2	cellular response to stimulus	Yes	5.01 / 18391.98	
AGCL1113Ccontig1	4.71	1.92E-03	2.3	4.94E-02	0.14	2.92E-03	NA		0	Very small peptide	
AG-N01F_023_J15	4.71	5.29E-07	11.7	3.03E-05	28.29	4.31E-03	basic blue copper protein	oxidation-reduction process	Yes	9.82 / 10324.85	
AG-R01F_032_F18	4.56	3.81E-06	2.5	1.20E-02	0.42	5.29E-03	cytochrome P450	oxidation-reduction process	Yes	ND	
AG-R01F_020_G10	4.41	3.52E-07	5.9	9.86E-05	0.11	1.52E-02	germin like protein.5		0	Yes	ND
AG-N01F_006_G15	4.37	6.67E-07	2.7	4.29E-04	0.91	7.86E-02	cationic peroxidase	oxidation-reduction process	Yes	ND	
AG-N01F_002_C06	4.34	6.70E-03	3.6	6.67E-03	125.38	7.39E-04	defensin cysteine rich antimicrobial protein, Ag3		0	Yes	9.36 / 6178.00
AGCL1514Ccontig1	4.19	1.79E-04	4.5	3.88E-03	0.36	4.66E-03	class IV chitinase	chitin catabolic process	Partial sequence	ND	
AG-J02F_002_N06	3.88	9.15E-06	4.0	2.54E-02	0.06	1.41E-02	class V chitinase	carbohydrate metabolic process	Partial sequence	ND	
AG-R01F_019_G06	3.64	2.46E-05	2.1	3.41E-02	16.08	1.32E-02	NA		0	?	
AG-R01F_001_A18	3.59	3.12E-07	4.5	2.70E-03	1.03	NS	Prp27-like protein		0	Yes	6.10 / 23102.67
AGCL169Ccontig1	3.29	4.34E-03	2.9	7.86E-03	12.42	2.83E-02	auxin-binding protein ABP20	cellular response to stimulus	Yes	ND	
AG-R01F_024_N21	3.14	4.19E-06	3.5	4.05E-03	1.11	NS	Prp27 like protein		0	Partial sequence	
AG-N01F_036_I04	3.03	2.01E-05	3.6	1.09E-03	1.10	NS	Prp27 like protein		0	Partial sequence	
AGCL194Ccontig1	2.99	5.21E-05	3.9	9.30E-05	0.92	NS	germin like protein.5	cellular response to stimulus	Yes	6.07 / 21323.34	
AGCL164Ccontig1	2.81	2.39E-05	2.5	2.47E-02	2.70	1.03E-02	glutathione S-transferase		0	No	
AG-N01F_024_P14	2.56	1.89E-04	2.4	3.49E-02	0.45	1.20E-02	cationic peroxidase	oxidation-reduction process	Partial sequence	ND	
AGCL191Ccontig1	2.50	4.18E-05	2.5	1.21E-02	0.83	NS	Prp27 like protein		0	Yes	5.79 / 23032.54
AGCL1559Ccontig1	2.45	8.83E-05	2.9	1.87E-02	7.18	2.70E-03	mannitol dehydrogenase	oxidation-reduction process	Partial sequence	ND	
AG-J02F_002_F23	2.37	8.29E-06	2.4	4.34E-05	1.77	NS	NA		0	Small sequence	
AG-N01F_037_C05	2.26	9.10E-05	38.9	2.25E-05	1.97	6.01E-03	receptor protein kinase perk1 like protein	cellular response to stimulus	No	ND	
AG-R01F_012_L02	2.12	1.18E-02	2.3	3.32E-03	0.22	3.61E-05	phenylalanine ammonia-lyase		0	Partial sequence	
gl_38453640_emb_A420771.1	2.18	9.83E-03	2.31	3.66E-03	ND	ND	phenylalanine ammonia-lyase		No	ND	

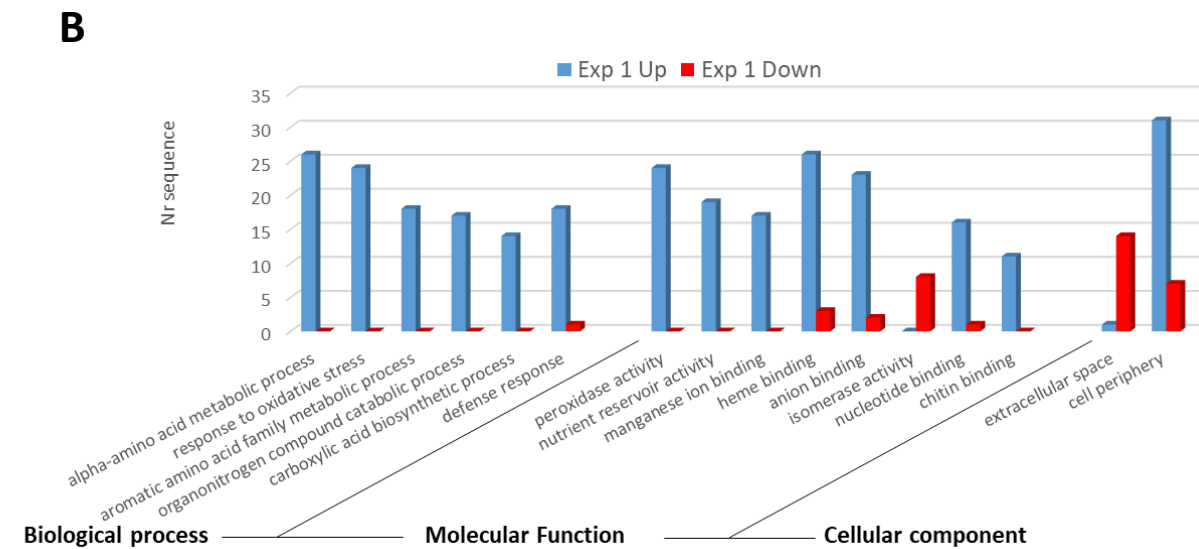
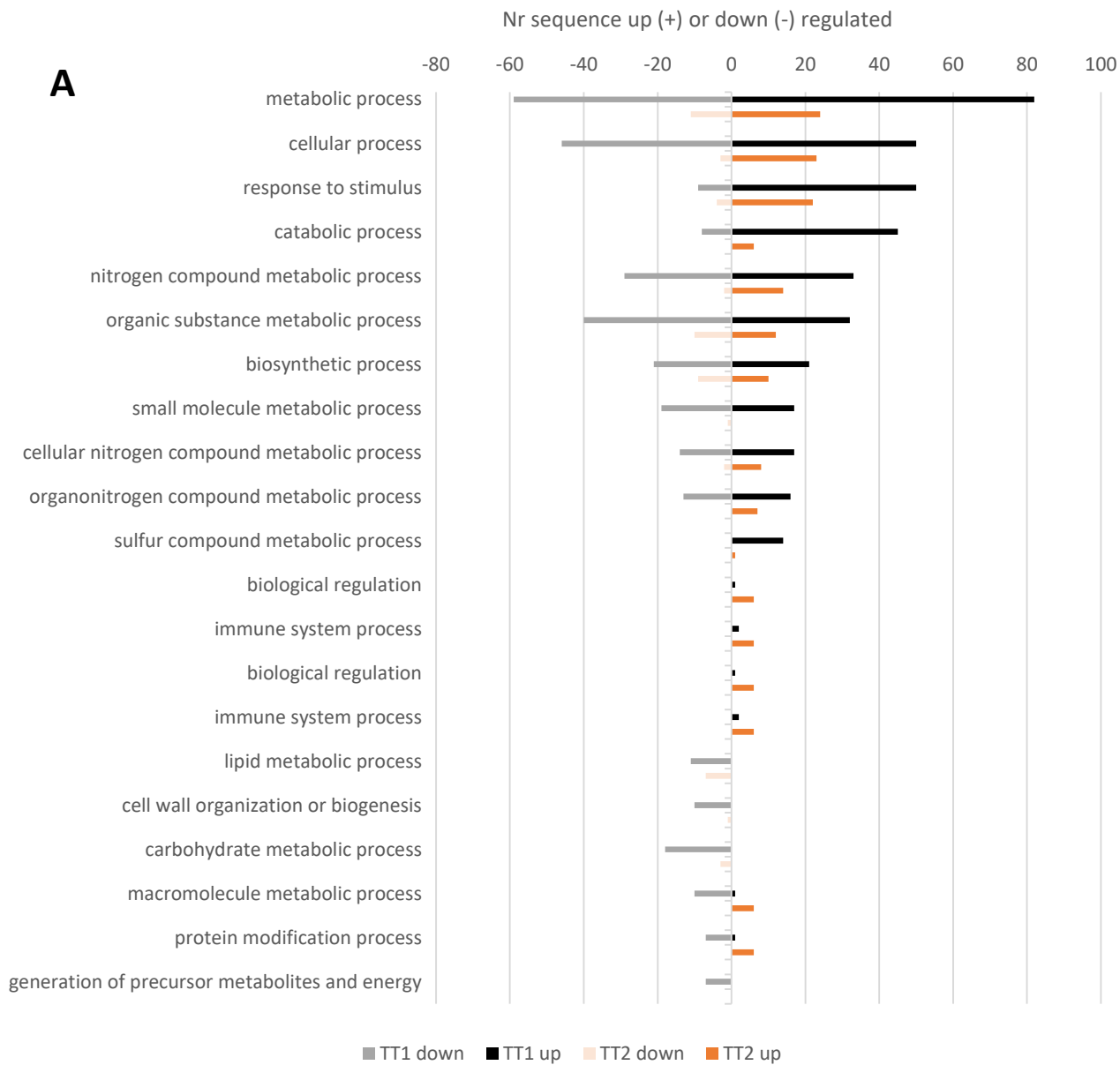


Figure 1: Gene Ontology (GO) functional classification analysis. A. Distribution of annotated genes into functional categories according to GO biological process. B. GO functional classification analysis was made by comparing (A) up and down-regulated genes found in Exp1 (Table S2) according to biological process, molecular function and cellular component through Fisher test. Number of sequences (Nr) were indicated for each category. BLAST2GO pipeline was used to get this GO annotation.

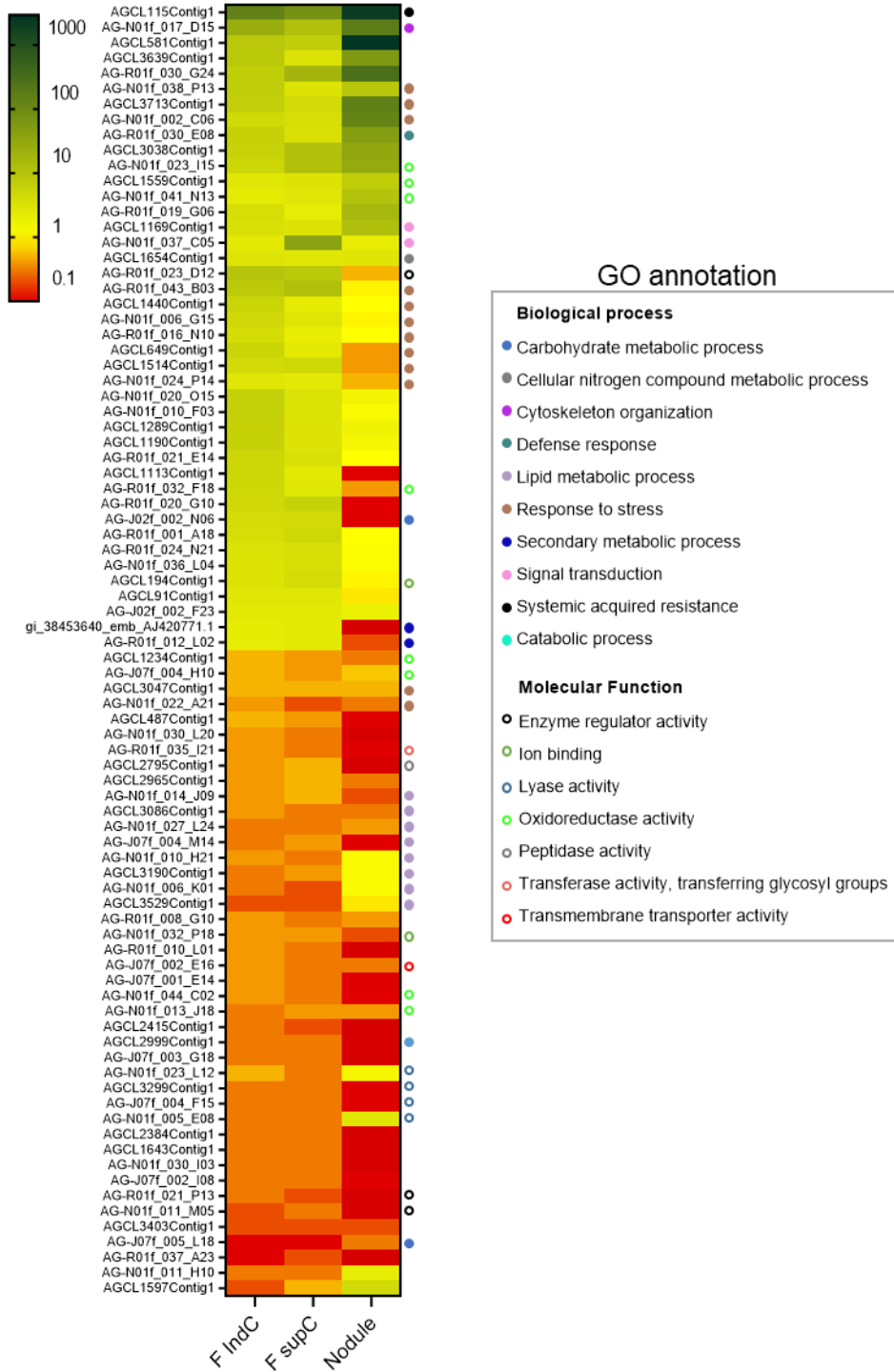


Figure 2: Expression levels of the genes which were commonly upregulated and downregulated in *FindC* and *FsupC* conditions. The expression level values in nodule were extracted from our previous work ((5); Table S4). The expression values were expressed as Fold change (FC) with a color gradient from red (down-regulated; ≤ 0.5) and orange-yellow (no-regulated) to green (up-regulated; ≥ 2) in infected roots or nodules compared to control roots without *Frankia*. The GO annotations were assigned by noting preferentially biological process and if not present, the molecular function. Certain genes have no GO assignment after blast2Go analysis. The heatmap was generated by GraphPad Prism 9.2.0.

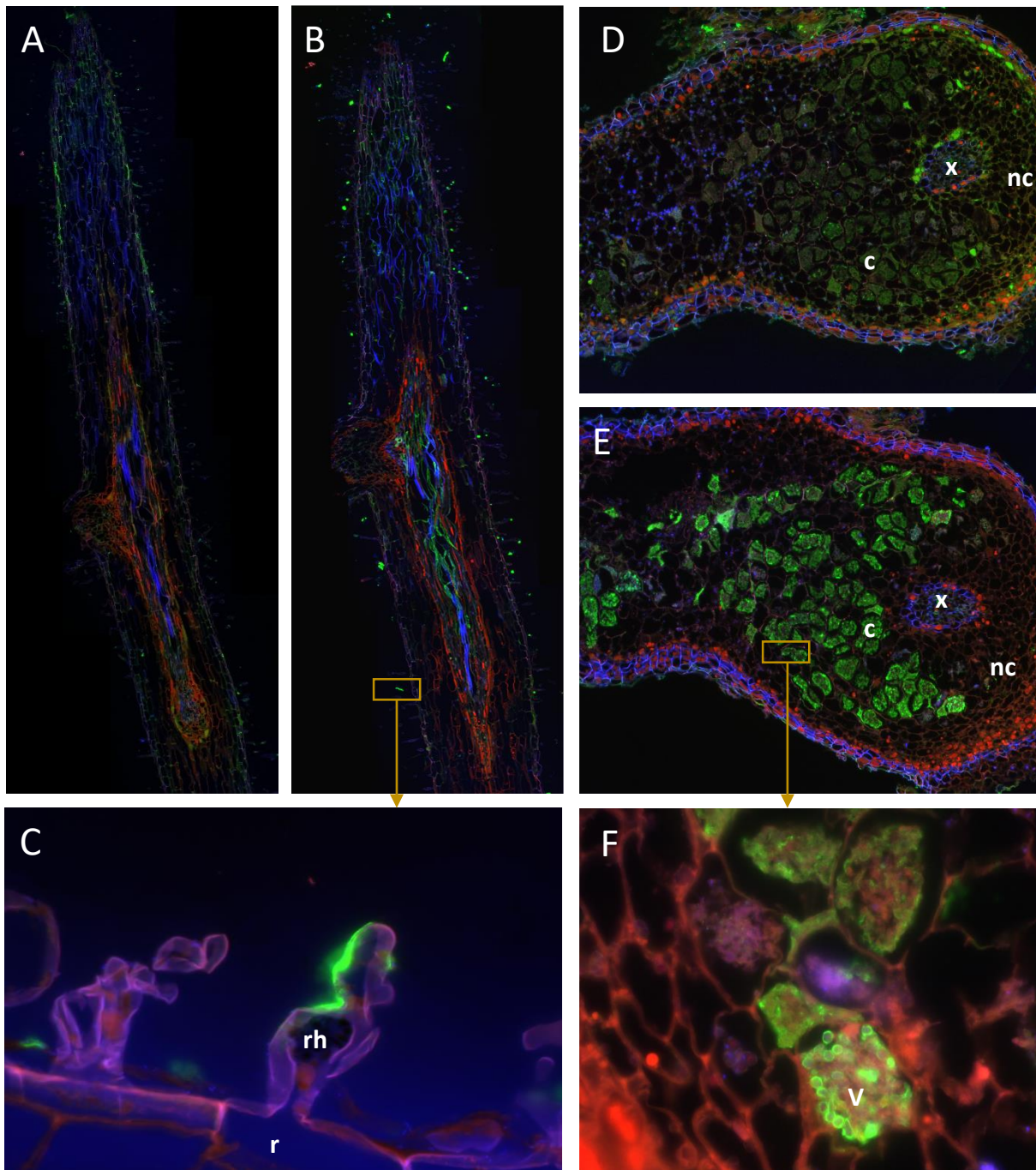


Figure 3: AgLTP24 localisation in roots after 2.5 days (A, B,C) or nodule of 21 dpi (D, E, F). Hair magnification of a specific zone of the infected root (C) or nodule (F). Immunofluorescence localization of AgLTP24 in hairy roots (B, C) and around *Frankia* vesicles in infected cells (E and F). Negative control with rabbit serum before intramuscular injection of AgLTP24 epitope (A, D) showed no green fluorescence in hairy roots (A) or infected cells (D).

Blue: DAPI; red: autofluorescence; green: Alexa Fluor 488 dye anti-rabbit antibody (Life Technologies, Saint Aubin, France). c, infected cells; nc, noninfected cells; v, *Frankia* vesicles; x, xylem.

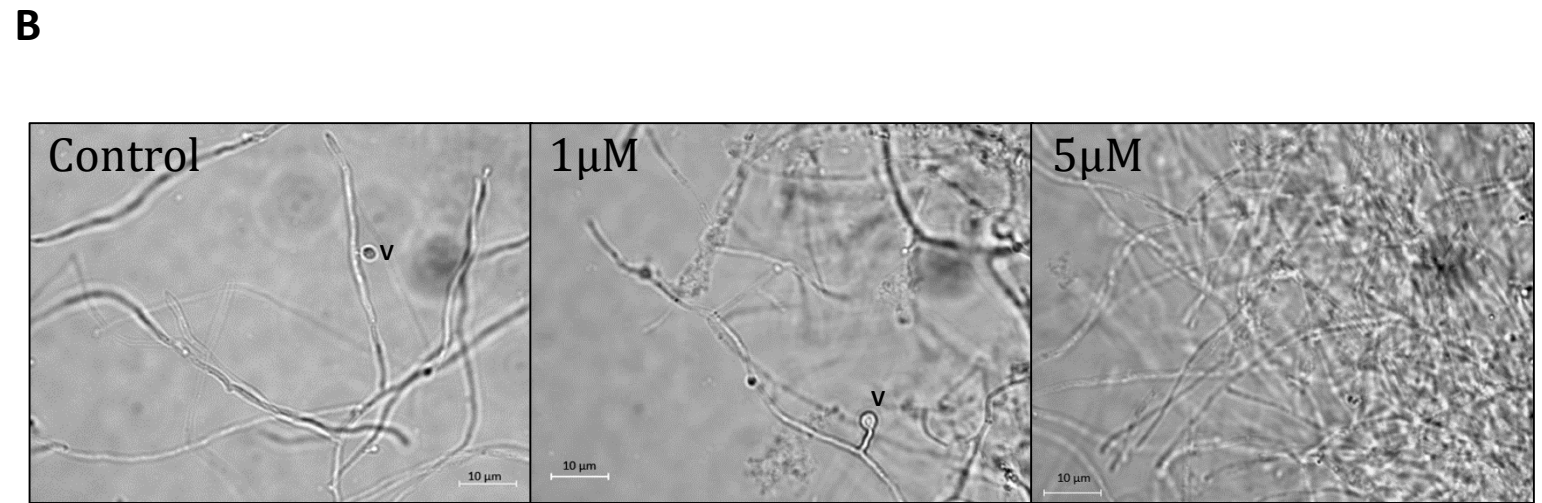
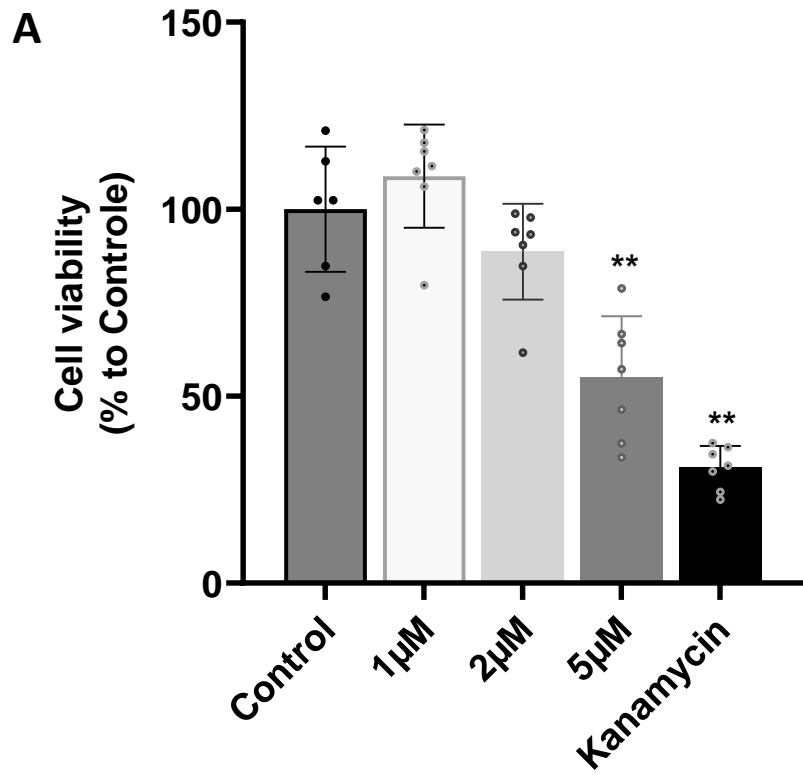


Figure 4: physiological bioassays on *Frankia* growth and cellular development. **A.** Resazurin bioassay on *Frankia* ACN14a growth after supplementation of 1 to 5 μM of AgLTP24. Cell viability was calculated by normalizing the fluorescence of the assay with the mean of the negative control (*Frankia* without AgLTP24). Kanamycin (40 μg.ml⁻¹) was used as positive control. Data are expressed as mean values ± SD. Differences between normalized data were assessed by the Mann Whitney test (bilateral and unpaired) compared to control. Graphic representation and statistical analysis of results was conducted with GraphPad Prism version 9.2.0. *p value <0.05, **p value <0.01. **B.** *Frankia* cells observation without or with gradual concentration of AgLTP24 from 0 (Control) to 5 μM and obtained during the different physiological bioassays. v, *Frankia* vesicles

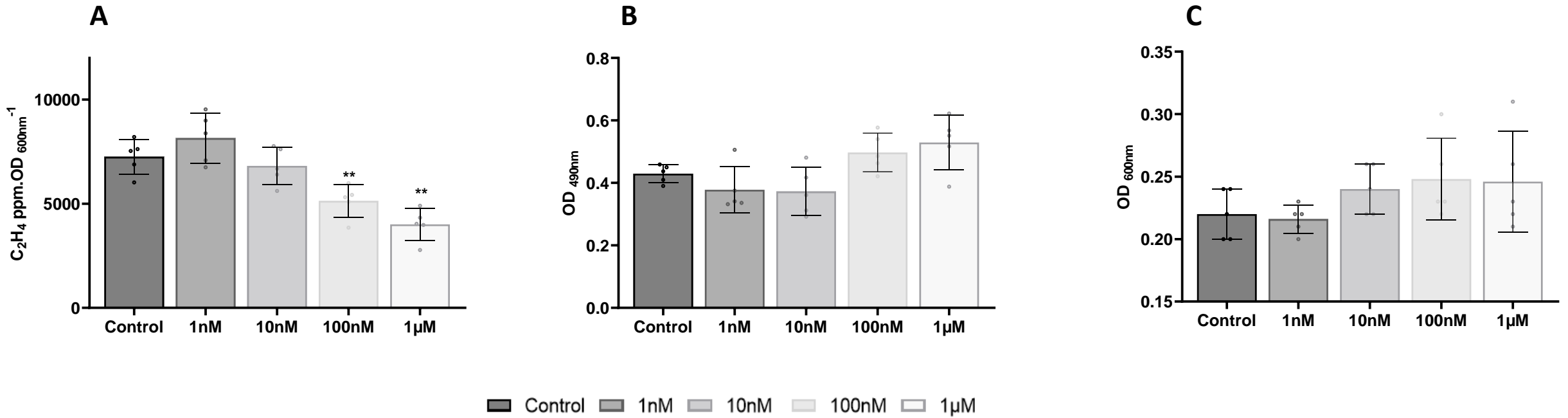


Figure 5: effect of AgLTP24 in physiology of *Frankia* after 7 days of growth on A. Nitrogen fixation; B. respiratory activity and C. growth by measuring OD_{600nm}. Data were extracted from the kinetic assay (Fig. S5). Data are expressed as mean values \pm SD. Differences between means were assessed by the Mann Whitney test (bilateral and unpaired) compared to control. Graphic representation and statistical analysis of results was conducted with GraphPad Prism 9.2.0. * p value < 0.05 , ** p value < 0.01 .

SUPPLEMENTAL DATA

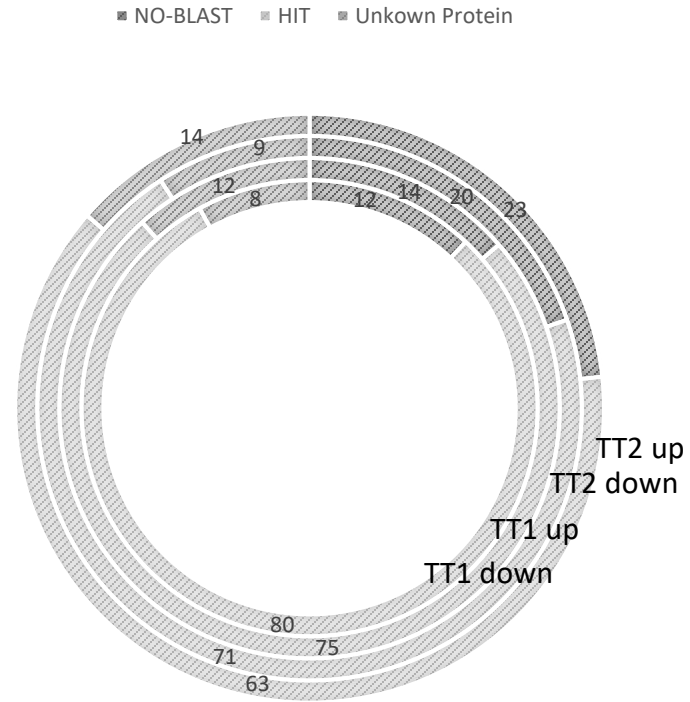


Figure S1: Gene Ontology (GO) analysis. Percent of distribution of genes giving a functional annotation (Hit), annotated as unknown protein and those yielding no blast.

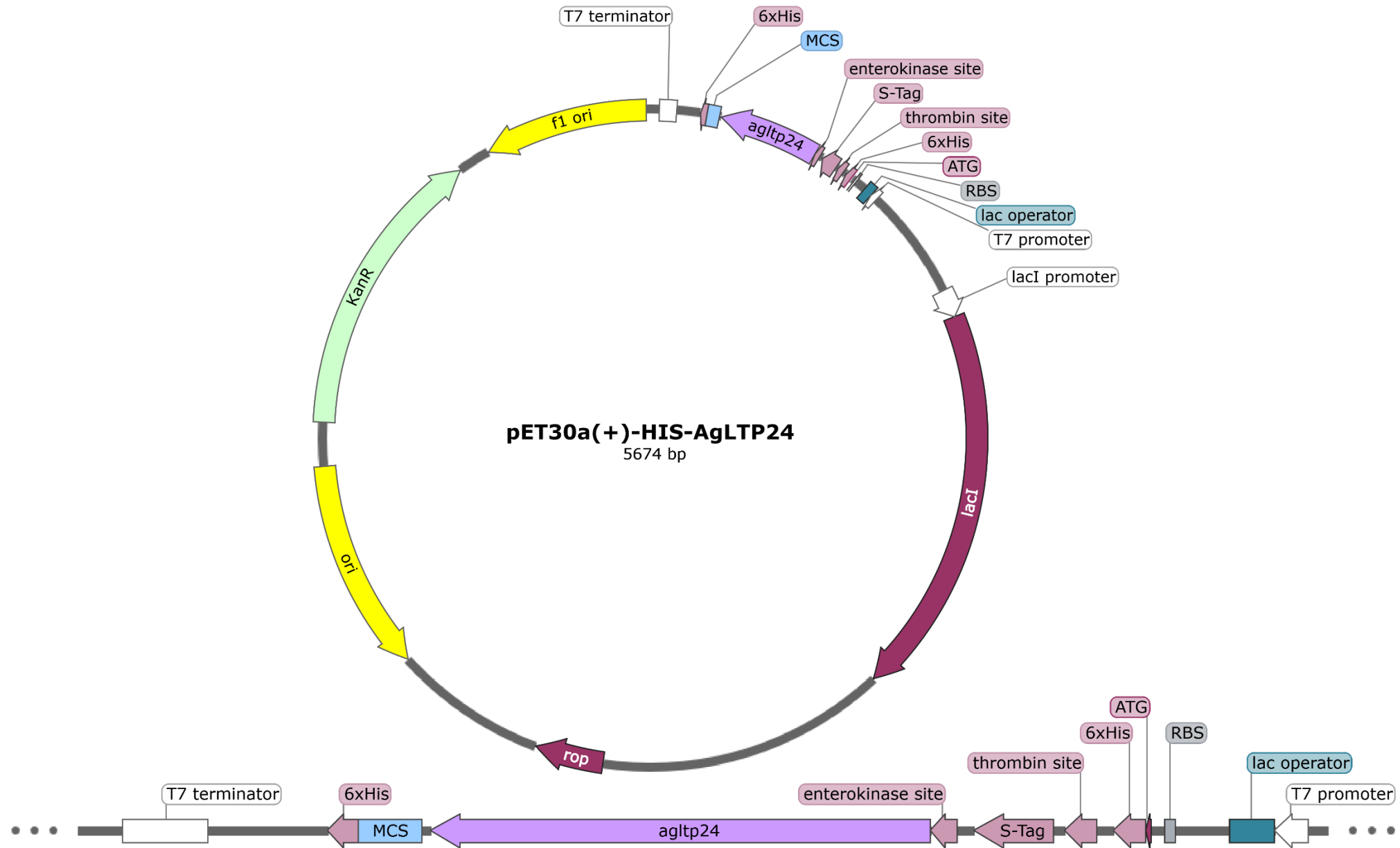


Figure S2: genetic map of the plasmid used to express AgLTP24 in *E. coli*.

KanR: Kanamycin resistance coding sequence, MCS: multiple cloning sites, 6xHis: HisTag coding sequence, *agltp24*: AgLTP24 mature peptide coding sequence.

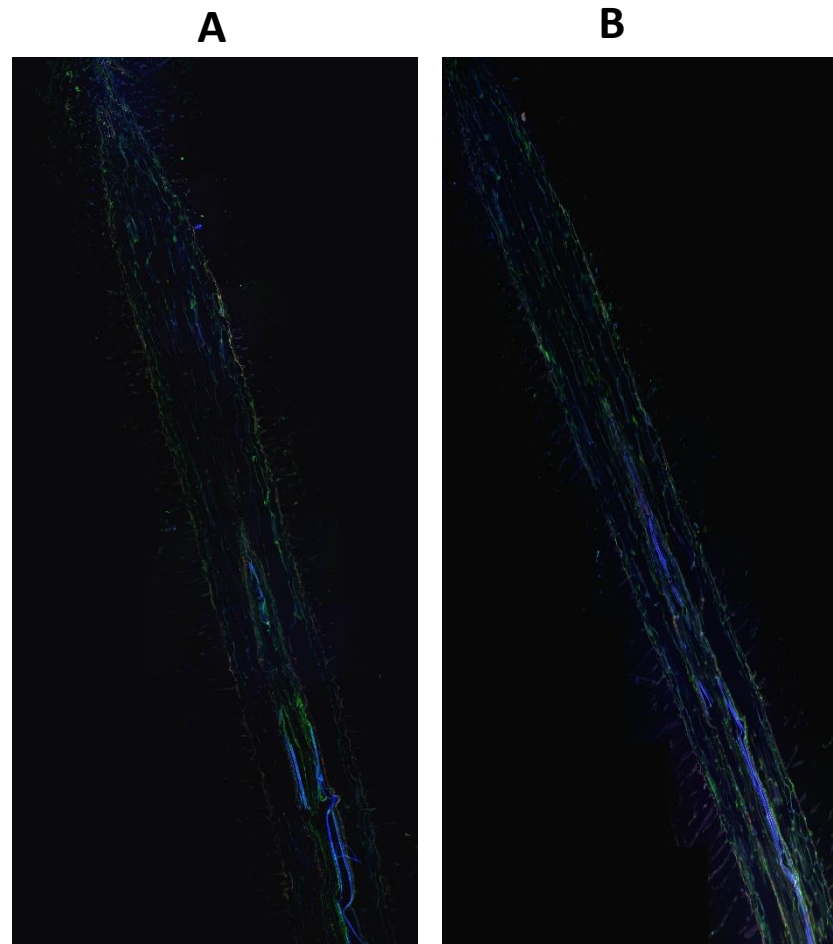


Figure S3: Negative control of immunolocalisation on non- infected roots using A. antibodies anti-AgLTP24 or B. rabbit serum obtained before intramuscular injection of AgLTP24 epitope. Blue: DAPI; red: autofluorescence; green: Alexa Fluor 488 dye anti-rabbit antibody (Life Technologies, Saint Aubin, France).

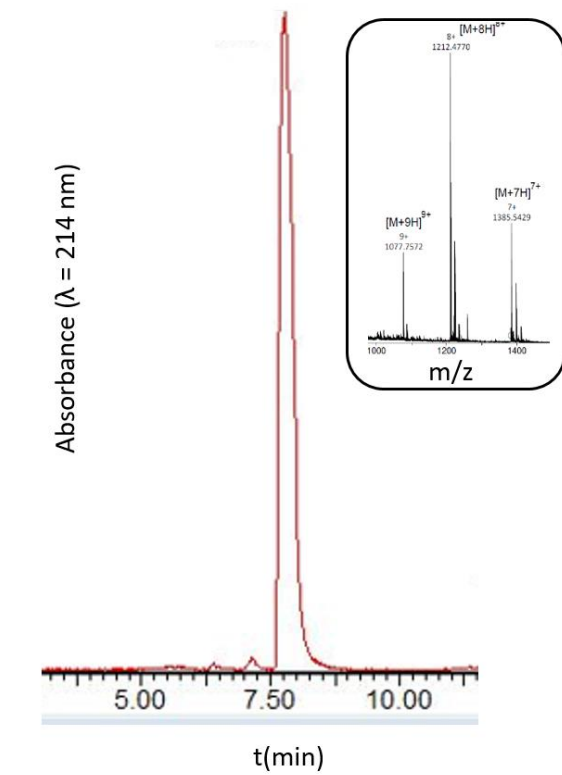


Figure S4: RP-UPLC chromatogram and ESI-HRMS mass spectrum of the purified folded AgLTP24 protein

Control 1 nM 10 nM 100 nM 1 μ M

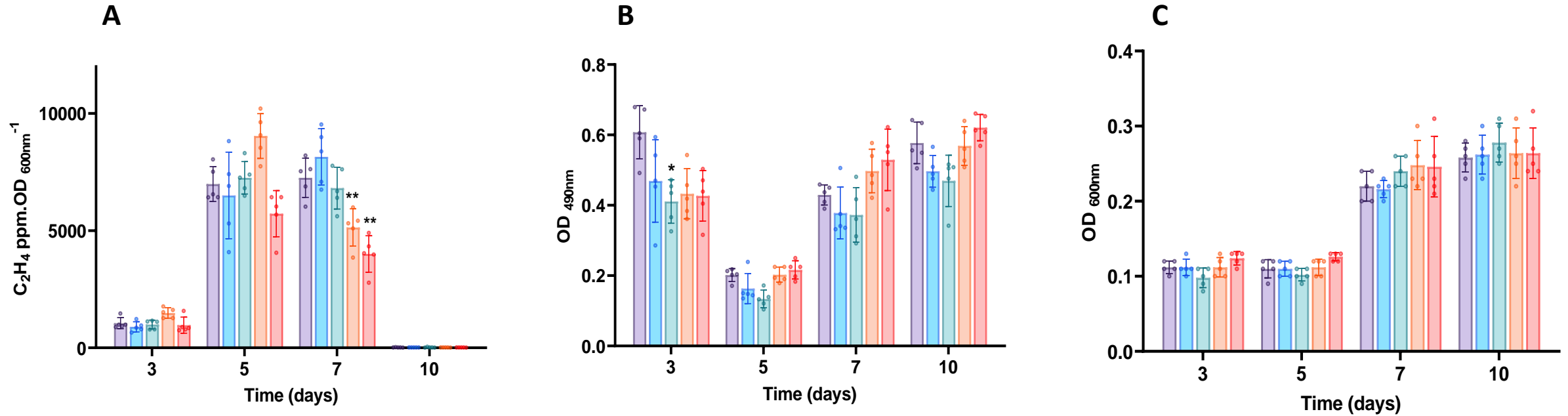


Figure S5: kinetic assay of *Frankia* ACN14a after addition of LTP24. Effects on A. nitrogen fixation through ARA activity B. respiratory activity through IRA and C. growth as OD 600nm level.

Data are expressed as mean values \pm SD. Differences between means were assessed by the Mann Whitney test (bilateral and unpaired) compared to control. Graphic representation and statistical analysis of results was conducted with GraphPad Prism version 9.2.0 (GraphPad software Inc; San Diego, CA, USA). * p value <0.05 , ** p value <0.01 .

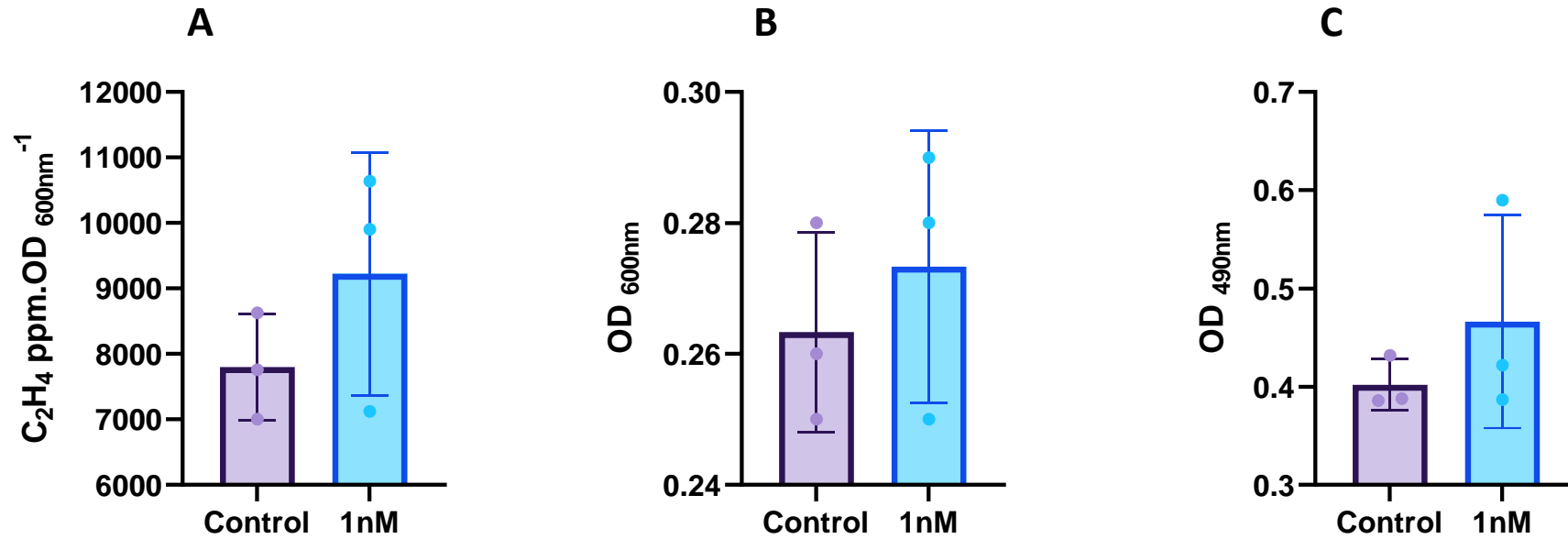


Figure S6: kinetic assay of *Frankia ACN14a* after addition of 1nM of LTP24. Effects on **A.** nitrogen fixation through ARA activity **B.** and **C.** respiratory activity through IRA.

Data are expressed as mean values \pm SD. Differences between means were assessed by the Mann Whitney test (bilateral and unpaired) compared to control. Graphic representation and statistical analysis of results was conducted with GraphPad Prism version 9.2.0 (GraphPad software Inc; San Diego, CA, USA). * p value <0.05 , ** p value <0.01 . growth through OD 600nm